Exploring mechanical properties of fully compostable flax reinforced composite filaments for 3D printing applications

Céline Badouard, Fanny Traon, Clément Denoual, Claire Mayer-Laigle, Gabriel Paës, Alain Bourmaud

Exploring mechanical properties of fully compostable flax reinforced composite filaments for 3D printing applications

[1]Céline Badouard, [1]Fanny Traon, [1]Clément Denoual, [2]Claire Mayer-Laigle, [3]Gabriel Paës, [1]Alain Bourmaud

(1) Univ. Bretagne Sud, UMR CNRS 6027, IRDL, F-56100 Lorient, France

(2) UMR 1208 IATE, Cirad, Inra, Montpellier SupAgro, University of Montpellier, 2, place Pierre Viala, 34060 Montpellier Cedex 02, France

(3) Fractionnement des AgroRessources et Environnement (FARE) laboratory, INRA, Université de Reims Champagne-Ardenne, 2 esplanade Roland Garros, 51100 Reims, France

Abstract

Plant fibres are increasingly used for composite reinforcement, but valorization of by-products such as flax shives still needs to be developed. Also, additive manufacturing, such as Fused Deposition Modelling (FDM), is strongly progressing and can be of great interest to implement biocomposite solutions. The present work focuses on the development of innovative and fully biodegradable filaments for FDM. Three polymer matrices were tested: PLLA, PLLA/PBS 50/50 %-wt and PBAT. A filler content of 30-wt% has been achieved using flax shives with PBAT. Flax fibres and shives reinforced 3D printed parts exhibit promising performances and printability, highlighting their potential to successfully develop fully compostable filaments.

Key-words: Fused Deposition Modelling; Biocomposites; Flax fibres; Flax shives; Mechanical properties

1. Introduction

Reinforcement of thermoplastic polymers with plant fibres is constantly increasing due to their high mechanical or environmental potential (Bourmaud et al., 2018). Biocomposites can be implemented by injection moulding, compression and the promising concept of 3D printing (Bourmaud et al., 2018). Their mechanical properties mainly depend on plant fibre type, aspect ratio (length/diameter) and quality of interface between the reinforcement and the polymer matrix. An important drawback of plant fibres is their moderate thermal resistance, potentially responsible for a decrease of the composite properties due to the thermo-mechanical shear rate occurring during the process (Bourmaud et al., 2018). The choice of the polymer matrix is a key point for obtaining high quality manufactured final product, which will strongly determine the quality of the interface with fibres and the process temperature, which must remain moderate (between 100-160 °C) in order to preserve the properties of the plant walls.

Fused Deposition Modelling (FDM), is a 3D printing technique enabling the manufacture of objects from digital 3D model data, usually layer-by-layer. 3D printing and especially FDM has attracted attention in the last years due to its high speed technique to produce parts with complex shape and geometry. Moreover, it is currently the most commonly used additive manufacturing technique due to the wide range of materials possibly used, from neat thermoplastics to composites and even biocomposites (Wang et al., 2017). One of the restricting factors for biocomposites manufacturing, and especially for 3D printing, is the incorporation of plant fibres. Recently, the possibility to use milled biobased products (such as miscanthus, seashell or rice husk) was demonstrated, using 3D printing machines with inkjet print heads. In this case, morphology and preparation of powder are the main key points to obtain performing composites (Zeidler et al., 2018). For FDM applications, size of particles is also a technological bottleneck regarding 3D printer nozzle size (generally between 0.4 and 1.0 mm) which implies an intense milling step. Indeed, grinding processes can lead to high heterogeneity and a loss in the mechanical properties of the composite (Berthet et al., 2017) mainly due to the decrease of the fibre aspect ratio. Specific techniques were developed to adapt the mechanical stress generated by the milling machines to the properties of the raw materials and hence to modulate the properties of the obtained powders (Motte et al., 2017). Moreover, dry separation techniques, such as electrostatic or triboelectric separation enable to regulate the particle properties such as particle size and shape distribution, spreading of these distributions, composition and surface properties of the particles (Mayer-Laigle et al., 2018). Finally, the filler dispersion and the crystallinity must be controlled to ensure a good-quality printing, especially regarding the shrinkage behaviour during the cooling step. In this context, most of the polymers used for FDM are amorphous or display a reduced crystallinity index (Benwood et al., 2018) to limit shrinkage and preserve polymer properties, inter-layer deposition and final part homogeneity. Finally, for biocomposites, the fibre volume fraction is also an important parameter. Impact of wood fibre content on PLA-wood filaments was studied and showed a decrease in tensile strength of the filaments due to the presence of higher void quantities and fibre clusters (Kariz et al., 2018).

The purpose of the present study is to investigate the development of 3D printable biocomposites reinforced with flax fibre and shives by comparing the mechanical properties of injected and 3D printed tensile specimens prepared with different matrices (PLLA for the reference, PBS and PBAT). The impact of the volume fraction and nature of the reinforcement, fibre or shive is also discussed.

2. Materials and methods

2.1 Materials

The flax fibre (*Linum usitassisimum L.*) used in this study is from the Alize variety (harvested in 2014) and was cultivated in Normandy (France). After dew retting and industrial scutching, flax fibres were cut at 1 mm length; the tensile Young's modulus, strength and elongation at break of the elementary scutched flax fibres were 53.8 ± 14.3 GPa, 1215 ± 500 MPa and 2.24 ± 0.59, respectively. Shives were first precrushed using a SM 300 knife mill with a 0.5 mm grid (Retsch, France) then fine milled with an UPZ impact mill with a 0.3 mm grid (Hosokawa Alpine®, Germany). The particle size distribution of shives and fibres was determined by laser diffraction using a laser diffraction particle size analyser Hydro 2000S (Malvern Instruments Ltd., United Kingdom) with liquid ethanol (ethylic alcohol: 96% v/v) carrier to avoid particle swelling. Three biodegradable polymers were used as matrices: Poly-(lactid) PLLA (7001D, Nature Works), Poly-(butyl-adipate-terephthalate) PBAT (Ecoflex® F Blend C1200, BASF) and Poly-(butylene-succinate) PBS (Bionolle 1020 MD, Showa Denko).

2.2 Processing

All raw materials were dried 15 hrs at 50 °C prior to the extrusion step to remove water. The formulated compounds were PLLA-10%-wt flax fibres (PLLA-10-F), PLLA/PBS 50/50-10%-wt flax fibres (PLLA-PBS-10-F), PLLA/PBS 50/50-10%-wt flax shives (PLLA-PBS-10-S) and PBAT-flax fibres at 10, 20 and 30%-wt (PBAT-10-F, PBAT-20-F and PBAT-30-F). All batches were compounded with a Bradender twin screw extruder at 20 rpm and 190 °C for PLLA composites and 150 °C for PBAT composites. The extruded composites were then granulated to obtain pellets, which were also dried at 50 °C and then injected to produce tensile specimens with a Battenfeld HM 80/210 injection press. Pellets were then extruded using a single-screw Scamex extruder (L/D = 20 and die diameter = 4 mm) to produce the filament. Filament thickness was adjusted to 2.85 ± 0.1 mm with a controlled diameter using a Zumbach 18 XY dual axis laser measuring head. 3D Printing was made using a Prusa i3 Rework 3D printer with Simplify 3D software and equipped with a 1.0 mm nozzle and an extrusion temperature of 190°C and 150°C for PLLA and PBAT composites, respectively. For all blends, printing speed and Z amplitude varied from 0.8-1.5 $m.min^{-1}$ and 0.6-1.0 mm, respectively. All blends with 10 wt% flax were quite simple to process, by both extrusion or printing step. Due to higher fibre fraction used with PBAT matrix, appearance of a shark skin phenomenon was noticed during filament manufacturing for 20%-wt and 30%-wt flax fibre loadings. In addition, for PBAT-30-F-I3D, some variations in extrusion flow rate were observed during 3D printing due to the increase of viscosity induced by higher fibre content. Then, tensile specimens were printed with a rectilinear filling pattern (100%) oriented at 0° with respect to the tensile direction. During all the printings, the printing surface temperature was maintained at 70°C.

2.3 Characterization

Tensile specimens were conditioned at room temperature (23°C and 48% relative humidity) for thermal and hygroscopic stability and characterized using MTS Synergie RT/1000 tensile machine with a 10 kN sensor according to the ISO 527 standard. These tests were performed using an extensometer (gauge length = 25 mm) and at crosshead speed of 1 mm/min and 50 mm/min for PLLA and PBAT matrices, respectively. Five dog bone specimens (180 x 10 x 4 mm) were analysed for each batch and average values of Young's modulus, stress at yield and elongation at break were determined. Raw fibres and shives were characterized by scanning electron microscopy (SEM) using a JEOL JSM 6460LV microscope at 20 kV. In addition, morphology of composites was examined. Tensile specimens were cut using an automatic saw and carefully polished to a 1-µm particle size finish solution. All samples were metallised with gold before being observed.

3. Results and discussions

3.1 Investigation of flax fibres and fines morphology

Figure 1 shows the particle size distribution of cut fibres and milled shives obtained by laser granulometry as well as SEM images of both reinforcements. Shives and fibres exhibit significant differences in size. Shives have a mono dispersed distribution with a peak at 220 µm and a median diameter value d(0.5) of 162 µm. Differing from results obtained with shives, size distribution of fibres evidences the presence of three peaks, with maximum values around 20 µm, 125 µm and 650 µm (Fig 1.A). This three-modal distribution was attributed to the response of the mathematical model of the particle size analyser applied to the diffraction image of flax elongated fibre. In addition, when a flax fibre batch is cut to produce short fibres, it was shown that (1) the main fibre fraction reached the targeted cut length and (2) the cutting process induces the production of the so-called fines particles, having a maximum length of 200 µm as defined by (Le Moigne et al., 2011). Figure 1.A confirms this specific behaviour of plant fibres, mainly due to destructuration of cell walls or to fibre length reduction induced by the presence of defects such as kink bands along the fibre length. Regarding SEM images, fibres seem to present homogenous lengths, which confirms that the distribution profile is an artefact due to the assumption of spherical particle made by the model used during laser particle size analysis. One can note that several fibres display a larger diameter. Indeed, within the flax stem, fibres are assembled into bundles which could remain cohesive after scutching, depending of the retting degree of the batch (Bourmaud et al., 2018).

3.2 Choice of the relevant polymer matrix

Table 1 gathers the measured mechanical properties for different injected and 3D printed samples. When flax fibres were added as reinforcements, all composite samples exhibited an increase in Young's modulus, regardless of the considered matrix and the processing tools used (injection or 3D printing). As previously

described (Tymrak et al., 2014), 3D printed mechanical properties of specimens are generally lower than those of injected ones due to presence of pores. Figure 2 shows cross sections of PLLA-10-F, PLLA-PBS-10-F and PBAT-10-F 3D printed specimens. Interestingly, whatever the considered matrix, inter-strand porosity is limited and the interface between printed layers are not clearly visible. However, porosities exist and are more numerous for PLLA-10-F sample which exhibits the highest tensile strength drop. Regarding the tensile strength of 3D printed or injected samples, values measured are always lower as compared to raw polymers except for PBAT matrix. Because of the important strain of this composites, these strength values are not representative of a common use of the material, these latter being generally used in a reduced range of elongation. For other formulations, injected composites exhibit tensile strength similar to raw polymers but a significant decrease was noticed for 3D printed parts with a loss of 35.7% and 18.5% for PLLA and PLLA-PBS blends, respectively. Tensile strength is dependent on the homogeneity and cohesion of composites and, even if printed materials had been subjected to a second extrusion step (for the implementation of the filament), this single screw melt could not be considered as an influencing compounding and homogenization step. Tensile strength is directly impacted by the presence of fibres bundles and also by large pores as observed on the PLLA-10-F sample. In the case of 3D printed composites, the reduced elongation at break, in comparison to the injected samples (Table 1), highlighted the presence of important defects such as porosities due to the printing step. Figure 4 confirms this statement by showing the important porosity fraction observed on 3D printed PLLA-10-F sample as compared to the injected ones, attributed to the specific layer-by-layer process and the filament manufacturing.

In addition to the clear correlation existing between strength values and presence of porosities within the samples, Young's modulus was also impacted. Indeed, a drop of 16.7%, 6.1% and 20.2% is observed for 3D printed PLLA-10-F, PLLA-PBS-10-F and PBAT-10-F, respectively, as compared to injection moulded samples. These differences are mainly due to the ability of the composites to be 3D printed and material parameters since stiffness, thermal properties and viscosity are of great interest for an efficient printability. Regarding pure PLLA, its high stiffness, improved when plant fibres are added, induces processing problems such as filament breakage or extrusion feeding instability. Low fibre contents may also be a drawback when flexible PBAT matrix is used, leading to irregularities in filament extrusion process, driving force or diameter control inducing instabilities during filament deposition. These difficulties during processing and printing favour the presence of porosities that have a clear effect on the mechanical performance of the printed parts. Mechanical performances are impacted by the mechanical properties of fibres and matrix and also by the orientation of the fibres and by the quality of the stress transfer between matrix and fibres; in case of high porosity content, the stress transfer is reduced and values of strength or stiffness greatly impacted.

3.3 Impact of the volume fraction and nature of the reinforcement

Finally, the influence of the fibre content was studied. PBAT material was selected due to its flexible behaviour , enabling higher loadings, with a relatively low melting temperature (about 115°C). Ideally, for 3D printing, obtaining a semi-rigid material is a need to favour winding and printing steps. PBAT was filled with 10, 20 and 30 wt% flax fibres. As the filler content increased in PBAT blends, the Young's modulus (Fig. 3A) and stress at yield (Fig. 3B) increased for both processes (FDM and injection moulding). The printed tensile specimens showed lower Young's modulus and stress at yield than those injected but remained significantly higher than the native material. These results demonstrated that it is possible to reinforce a flexible matrix up to 30%-wt flax fibres for 3D printing application. It only requires an increase of the printing temperature to fit the viscosity of the materials. As explain in the Materials and Methods section, a 1 mm nozzle was selected to print the specimen to avoid the formation of clusters formed for high fibre fractions. A 0.4 or 0.6 mm nozzle might possibly be used in future work through the optimization of both fibre dispersion and granulometry.

Finally, an alternative solution, using flax shives was explored. For these experiments, a PLLA-PBS matrix was chosen for its good compatibility with flax and its high elongation at break which makes it well suitable for 3D printing process. Length of shives is significantly smaller than fibres (Fig.1) and has consequently a reduced aspect ratio. Thus, Young's modulus of composite reinforced with shives was reduced as compared to those of PLLA-PBS-Flax fibres (Table 1). Interestingly, this latter was significantly higher than neat PLLA/PBS. As for the previous blends, Young's modulus of shives reinforced printed specimens was lower than injected ones but tensile strength values were in the same order for both injected and 3D printed samples. The smaller size of shives, as compared to fibres, is probably a significant advantage to improve the quality of 3D printed parts, due to a better dispersion of the reinforcement induced by the important shear rate occurring during the extrusion cycle needed to produce the filaments.

4. Conclusion

This work explored the use of flax fibers and shives to develop biodegradable filaments for 3D printing. It was shown that the choice of matrix is an important parameter to control the mechanical performance of the materials produced. Depending on their initial elongation, the considered polymers may accept more or less fibre volume fractions. Interestingly, PBAT appears to be a suitable candidate due to its flexibility. Finally, the crushed flax shives demonstrated their potential in reinforcing, providing high stiffness and strength when incorporated into a PLLA-PBS matrix and opening the way for a possible valorisation of these co-products of flax cultivation.

Acknowledgements

The authors want to acknowledge the French National Institute for Agricultural Research (INRA) for funding this work through the collaborative project FLUOFLAX4D.

Bibliography

Benwood, C., Anstey, A., Andrzejewski, J., Misra, M., Mohanty, A.K., 2018. Improving the Impact Strength and Heat Resistance of 3D Printed Models: Structure, Property, and Processing Correlationships during Fused Deposition Modeling (FDM) of Poly(Lactic Acid). ACS Omega 3, 4400–4411. doi:10.1021/acsomega.8b00129

Berthet, M.-A., Mayer-Laigle, C., Rouau, X., Gontard, N., Angellier-Coussy, H., 2017. Sorting natural fibres: A way to better understand the role of fibre size polydispersity on the mechanical properties of biocomposites. Compos. Part A Appl. Sci. Manuf. 95, 12–21. doi:https://doi.org/10.1016/j.compositesa.2017.01.011

Bourmaud, A., Beaugrand, J., Shah, D.., Placet, V., Baley, C., 2018. Towards the design of high-performance plant fibre composites. Prog. Mater. Sci. 97, 347–408.

Kariz, M., Sernek, M., Obućina, M., Kuzman, M.K., 2018. Effect of wood content in FDM filament on properties of 3D printed parts. Mater. Today Commun. 14, 135–140. doi:https://doi.org/10.1016/j.mtcomm.2017.12.016

Le Moigne, N., Van den Oever, M., Budtova, T., 2011. .A statistical analysis of fibre size and shape distribution after compounding in composites reinforced by natural fibres. Compos. Part A Appl. Acience Manuf. 42, 1542–1550.

Mayer-Laigle, C., Barakat, A., Barron, C., Delenne, J.Y., Frank, X., Mabille, F., Rouau, X., Sadoudi, A., Samson, M.-F., Lullien-Pellerin, V., 2018. DRY biorefineries: Multiscale modeling studies and innovative processing. Innov. Food Sci. Emerg. Technol. 46, 131–139. doi:https://doi.org/10.1016/j.ifset.2017.08.006

Motte, J.-C., Delenne, J.-Y., Barron, C., Dubreucq, É., Mayer-Laigle, C., 2017. Elastic properties of packing of granulated cork: Effect of particle size. Ind. Crops Prod. 99, 126–134. doi:https://doi.org/10.1016/j.indcrop.2017.01.043

Tymrak, B.M., Kreiger, M., Pearce, J.M., 2014. Mechanical properties of components fabricated with open-source 3-D printers under realistic environmental conditions. Mater. Des. 58, 242–246. doi:https://doi.org/10.1016/j.matdes.2014.02.038

Wang, Z., Xu, J., Lu, Y., Hu, L., Fan, Y., Ma, J., Zhou, X., 2017. Preparation of 3D printable micro/nanocellulose-polylactic acid (MNC/PLA) composite wire rods with high MNC constitution. Ind. Crops Prod. 109, 889–896. doi:https://doi.org/10.1016/j.indcrop.2017.09.061

Zeidler, H., Klemm, D., Böttger-Hiller, F., Fritsch, S., Guen, M.J. Le, Singamneni, S., 2018. 3D printing of biodegradable parts using renewable biobased materials. Procedia Manuf. 21, 117–124. doi:https://doi.org/10.1016/j.promfg.2018.02.101

Table caption

Table 1. Tensile properties of raw polymers and flax fibres or shives reinforced composites with several of biodegradable matrices. Elongation at break of native PBAT cannot be obtained due to its excessive elongation. INJ = injected; 3DP = 3D printed; F = fibres and S = shives.

Figure caption

Figure 1. Size distribution (A) and SEM images of flax shives (B) and fibres (C). Scale bar is 500 µm.

Figure 2. SEM observation of composite cross section for 3D printed PLLA-PBS-10-F, PLLA-10-F and PBAT-10-F. Scale bar is 500 µm.

Figure 3. SEM observation on composite cross section for injected (A) and 3D printed PLLA-10-F (B) sample. Scale bar is 500 µm.

Figure 4. Evolution of tensile modulus (A) and strength (B) for injected and 3D printed PBAT-flax fibres composites.

Figure 1. Size distribution (A) and SEM images of flax shives (B) and fibres (C). Scale bar is 500 µm.

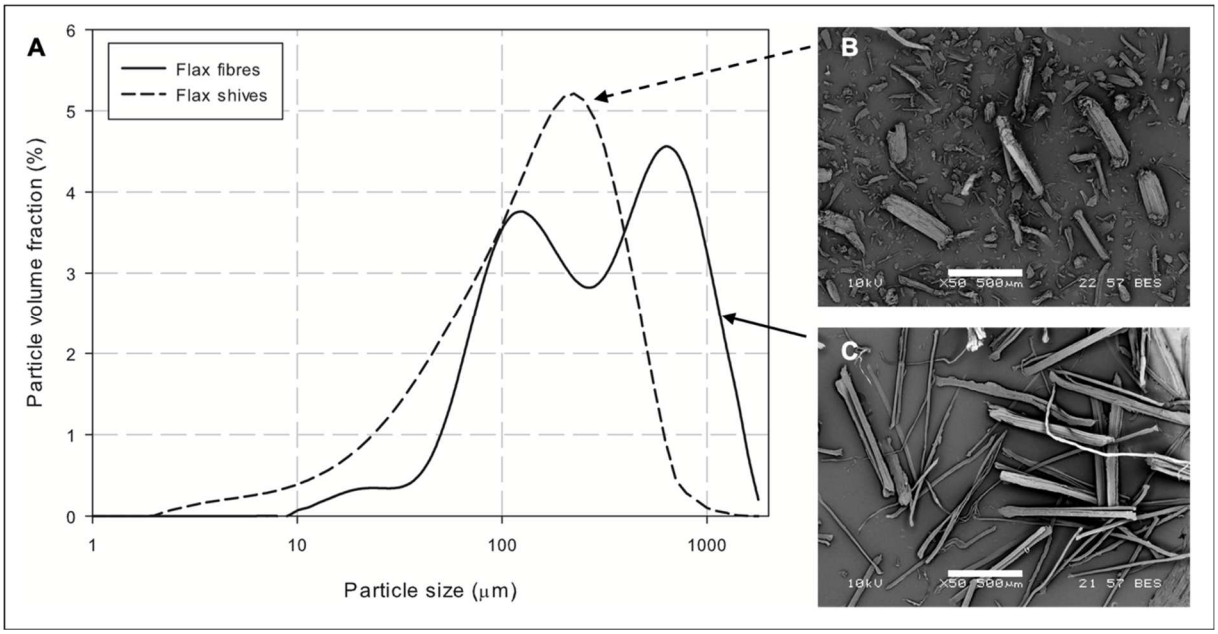

Figure 2. SEM observation of composite cross section for 3D printed PBAT-10-F, PLLA-10-F and PLLA-PBS-10-F samples. Scale bar is 500 µm.

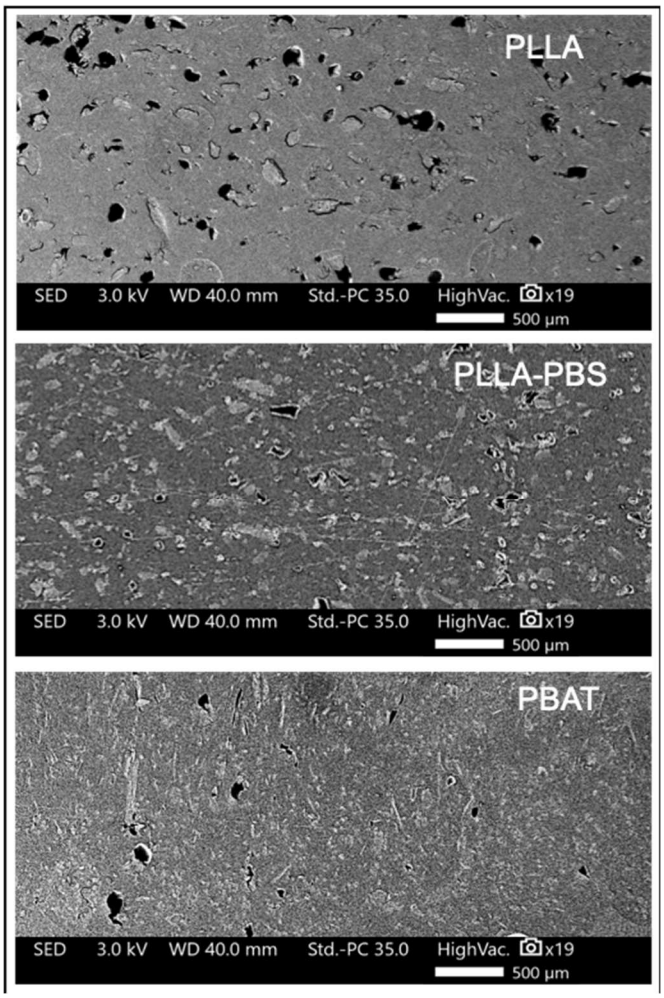

Figure 3. SEM observation of composite cross section for injected (A) and 3D printed PLLA-10-F (B) sample. Scale bar is 500 µm.

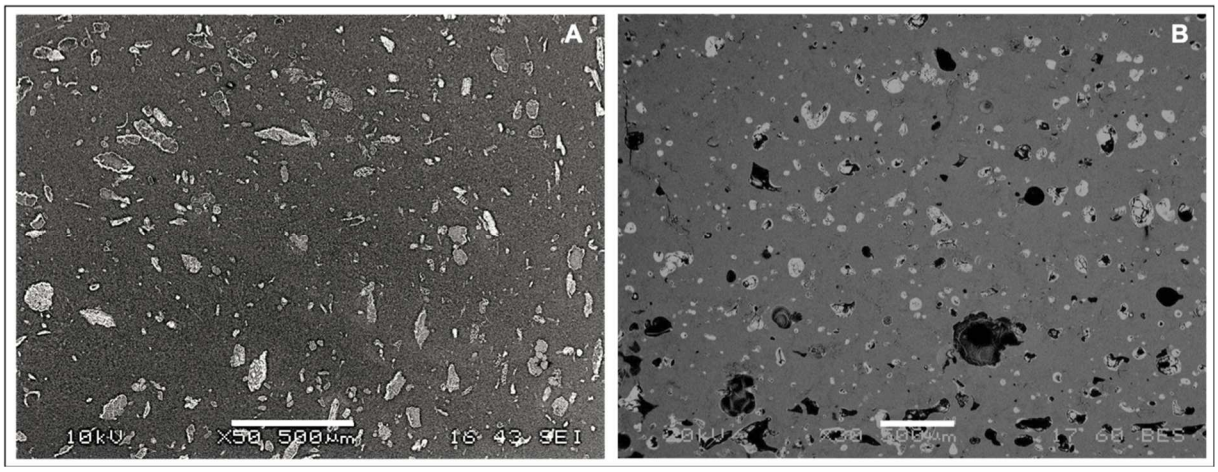

Figure 4. Evolution of tensile modulus (A) and strength (B) for injected and 3D printed PBAT-flax fibres composites.

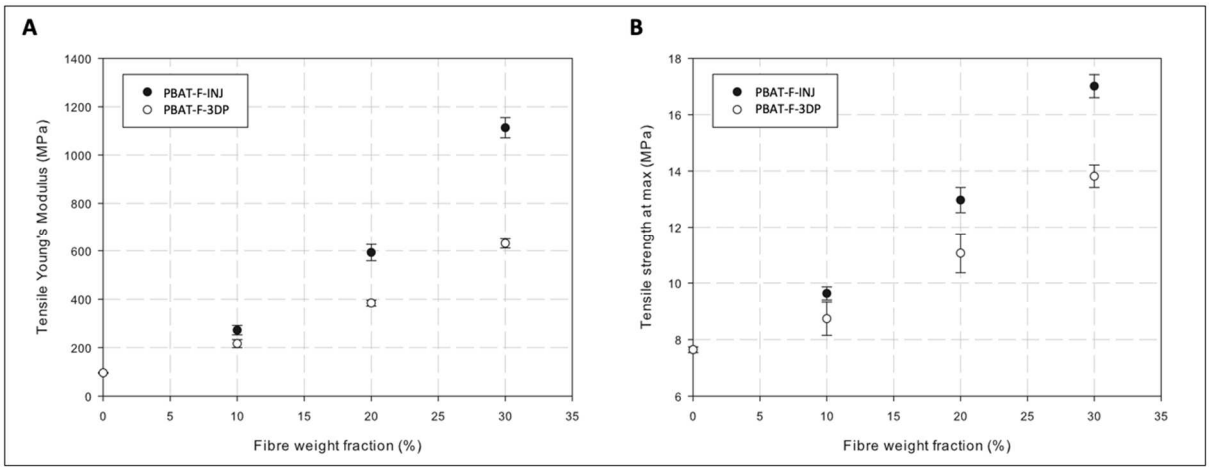

Table 1. Tensile properties of raw polymers and flax fibres or shives reinforced composites with several of biodegradable matrices. Elongation at break of native PBAT cannot be obtained due to its excessive elongation. INJ = injected; 3DP = 3D printed; F = fibres and S = shives.

Sample	Young's Modulus (MPa)	Strength at max (MPa)	Elongation at break (%)
PLLA-INJ	3760 ± 56	55.2 ± 0.9	2.8 ± 0.4
PLLA-10-F-INJ	4765 ± 166	53.2 ± 1.8	1.9 ± 0.2
PLLA-10-F-3DP	3968 ± 245	34.2 ± 2.6	1.2 ± 0.1
PLLA-PBS-INJ	2070 ± 83	39.1 ± 1.8	12.5 ± 2.2
PLLA-PBS-10-F-INJ	2968 ± 175	37.2 ± 0.1	3.3 ± 0.1
PLLA-PBS-10-F-3DP	2786 ± 251	30.3 ± 2.5	1.8 ± 0.4
PLLA-PBS-10-S-INJ	2573 ± 147	34.2 ± 3.4	2.1 ± 0.5
PLLA-PBS-10-S-3DP	2190 ± 114	34.1 ± 1.9	1.3 ± 0.2
PBAT-INJ	96 ± 2	7.6 ± 0.1	-
PBAT-10-F-INJ	272 ± 19	9.6 ± 0.2	312.1 ± 7.4
PBAT-10-F-3DP	217 ± 16	8.7 ± 0.6	364.1 ± 24.3